LA-4221-MS

C.2

LOS ALAMOS SCIENTIFIC LABORATORY
of the
University of California

LOS ALAMOS • NEW MEXICO

Heat Pipe Design Considerations

UNITED STATES
ATOMIC ENERGY COMMISSION
CONTRACT W-7405-ENG. 36

This report expresses the opinions of the author or authors and does not necessarily reflect the opinions or views of the Los Alamos Scientific Laboratory.

Text extracfed from LA-4109-MS

Distributed: August 1, 1969

LA-4221-MS
SPECIAL DISTRIBUTION

LOS ALAMOS SCIENTIFIC LABORATORY
of the
University of California
LOS ALAMOS • NEW MEXICO

Heat Pipe Design Considerations

by

Joseph E. Kemme

For presentation at the Eleventh Heat Transfer Conference, August 3-6, 1969, Minneapolis, Minnesota

HEAT PIPE SYSTEMS

Review of Heat Pipe Performance Characteristics

Introduction

During the past few years, experiments have been made at LASL to determine the operating characteristics and heat-transfer limitations of heat pipes. A review report is being prepared to provide a better understanding of the principles of heat-pipe operation and to show how these principles can be applied to improve their heat-transfer performance. Some of the information in the report is given in the following paragraphs.

Manner of Operation

A simple heat pipe consists of a sealed tube with its interior lined with a thin capillary network called a wick. The wick contains the liquid phase of a working fluid and the remaining space contains the vapor phase. This arrangement provides a distinct flow path for each phase, but the paths have a common liquid-vapor interface which allows them to communicate in all parts of the system.

When one part of the heat pipe is heated and another part cooled, a countercurrent two-phase flow cycle is established, with mass addition and mass extraction. Evaporation and condensation occur wherever the liquid-vapor interface exists, but there is a net rate of evaporation in the heated section. The excess vapor flows to the cooled section where it condenses on the wick surface and releases its latent heat of evaporation. This heat is removed by conduction through the saturated wick and container wall to the cooling environment. The condensate is drawn into the wick and returned to the heated section to complete the flow cycle.

Although a heat pipe behaves like a structure of very high thermal conductance, it possesses heat-transfer limitations which are governed by certain principles of fluid mechanics. The possible effects of these limitations on the capability of a heat pipe with a liquid-metal working fluid are shown in Fig. 1. Individual limitations indicated in the figure are discussed below.

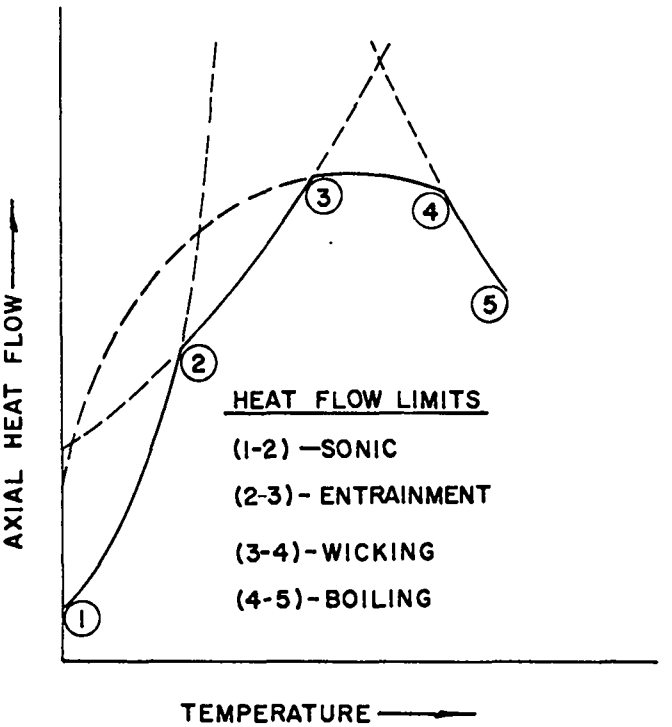

Fig. 1. Heat pipe limitations.

Sonic Limitation

When heat is transferred from the heated section (evaporator) of a heat pipe to the cooled section (condenser) the rate of heat transfer, Q, between the two sections is given by

$$Q = \dot{m}_v L, \qquad (1)$$

where $\dot{m}_v$ = rate of mass flow of vapor at evaporator exit, and L = latent heat of fluid. Because the latent energy of the working fluid is used instead of its heat capacity, rather large heat-transfer rates can be achieved with a relatively small mass flow. Furthermore, if the heat is transferred by high-density, low-velocity vapor, the transfer is nearly isothermal because small pressure gradients in the vapor support its motion.

To show the effect of vapor density and velocity on heat transfer, Eq. 1 can be modified

by using the continuity equation

$$\dot{m}_v = \bar{\rho}_v \bar{V} A, \qquad (2)$$

where $\bar{\rho}_v$ = radial average vapor density at evaporator exit, $\bar{V}$ = the average axial vapor velocity at evaporator exit, and A = cross-sectional area of vapor passage. By combining Eqs. 1 and 2 and rearranging, the result is

$$\frac{Q}{A} = \bar{\rho}_v \bar{V} L, \qquad (3)$$

where Q/A is the axial heat flux based on the cross-sectional area of the vapor passage.

As indicated by Eq. 3, the axial heat flux in a heat pipe can be held constant and the condenser environment adjusted to lower the pressure, temperature, and density of the vapor until the flow at the evaporator exit becomes sonic. Once this occurs, pressure changes in the condenser will not be transmitted to the evaporator. This sonic limiting condition is represented in Fig. 1 by the solid curve between Points 1 and 2. Some values for sonic heat-flux limits as a function of evaporator exit temperature are given in Table 1 for Cs, K, Na, and Li.

TABLE 1. SONIC LIMITATIONS OF HEAT-PIPE WORKING FLUIDS

Evaporator Exit Temperature, °C	Heat-Flux Limits, kW/cm^2			
	Cs	K	Na	Li
400	1.0	0.5	--	--
500	4.6	2.9	0.6	--
600	14.9	12.1	3.5	--
700	37.3	36.6	13.2	--
800	--	--	38.9	1.0
900	--	--	94.2	3.9
1000	--	--	--	12.0
1100	--	--	--	31.1
1200	--	--	--	71.0
1300	--	--	--	143.8

Although heat pipes are normally not operated at sonic flow, such conditions have been encountered during startup with the working fluids listed in Table 1. Temperatures during such startups are always higher at the beginning of the heat-pipe evaporator than at the evaporator exit. The difference in temperature can be predicted by using the momentum equation for a system with mass addition

$$P_1 = P_2 + \rho_v V^2, \qquad (4)$$

where P_1 = static pressure at beginning of evaporator, P_2 = static pressure at evaporator exit, and $\rho_v V^2$ = dynamic pressure at evaporator exit. If the velocity is expressed in terms of a Mach number, use of the ideal gas relationships gives

$$\frac{P_1}{P_2} = 1 + M^2 k, \qquad (5)$$

where M = Mach number at exit, and k = ratio of specific heats of vapor. The use of Eq. 5 and of appropriate vapor pressure-temperature curves allows the evaporator temperature gradients to be determined at sonic and subsonic conditions.

Entrainment Limitation

Ordinarily, the sonic limitations just discussed do not cause dryout of the wick with attendant overheating of the evaporator. In fact, they often prevent the attainment of other limitations during startup. However, if the vapor density is allowed to increase without an accompanying decrease in velocity, some liquid from the wick-return system may be entrained. The onset of entrainment can be expressed in terms of a Weber number

$$\frac{\rho_v V^2 \lambda}{2\pi\gamma} = 1, \qquad (6)$$

where λ = a characteristic length, and γ = liquid surface tension. Equation 6 simply expresses the ratio of vapor inertial forces to liquid surface tension forces. When this ratio exceeds unity, a condition exists very similar to that of a body of water agitated by high-velocity winds into waves

which propagate until liquid is torn from their crests. Once entrainment begins in a heat pipe, fluid circulation increases until the liquid-return path cannot accommodate the increased flow. This causes dryout and overheating of the evaporator.

Because the wavelength of the perturbations at the liquid-vapor interface in a heat pipe is determined by the wick structure, the entrainment limit can be estimated by combining Eqs. 3 and 6 to give

$$\frac{Q}{A} = \sqrt{\frac{2\pi \rho_v \gamma L^2}{\lambda}} \quad . \tag{7}$$

Equation 7 can then be used to obtain the type of curve represented by the solid line between Points 2 and 3 in Fig. 1.

Wicking Limitation

Fluid circulation in a heat pipe is maintained by capillary forces which develop in the wick structure at the liquid-vapor interface. These forces balance the pressure losses due to the flow in the liquid and vapor phases; they are manifest as many tiny menisci which allow the pressure in the vapor to be higher than the pressure in the adjacent liquid in all parts of the system. When a typical meniscus is characterized by two principal radii of curvature(r_1 and r_2) the pressure drop, ΔP_c, across the liquid surface is given by

$$\Delta P_c = \gamma \left(\frac{1}{r_1} + \frac{1}{r_2} \right) \quad . \tag{8}$$

These radii, which are smallest at the evaporator end of the heat pipe, become even smaller as the heat-transfer rate is increased. If the liquid wets the wick perfectly, the radii will be defined exactly by the pore size of the wick when a heat-transfer limit is reached. Any further increase in heat transfer will cause the liquid to retreat into the wick, and drying and overheating will occur at the evaporator end of the system.

As indicated by Eq. 8, the capillary force in a heat pipe can be increased by decreasing the size of the wick pores which are exposed to vapor flow. However, if the pore size is decreased also in the remainder of the wick, the wicking limit

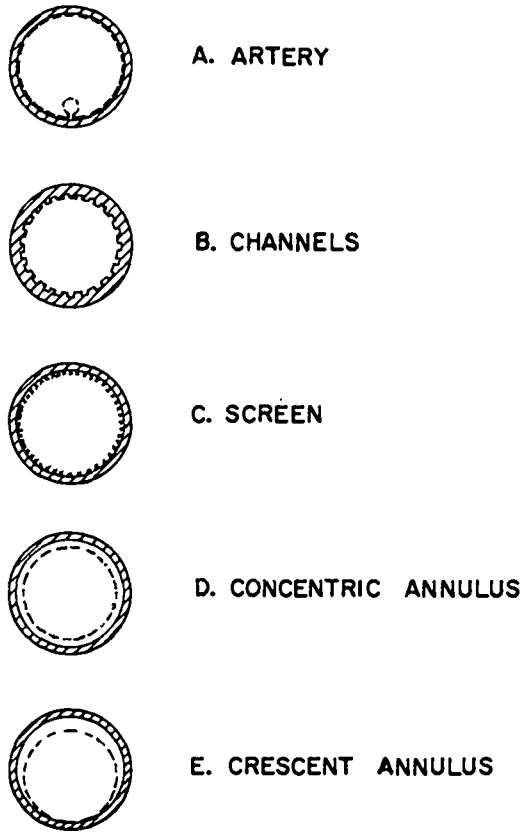

Fig. 2. Cross sections of various wick structures.

might actually be reduced because of the increased pressure drop in the liquid phase. This is shown by Poiseuille's equation for the pressure drop through a capillary tube

$$\Delta P_L = \frac{8\mu \dot{m}_L Z}{\pi r^4 \rho} \quad , \tag{9}$$

where μ = liquid viscosity, $\dot{m}_L$ = rate of mass flow of liquid, r = tube radius, ρ = liquid density, and Z = tube length.

Equation 9 can be modified to obtain the liquid-pressure drop at a particular heat-transfer rate, Q, for various wick structures. The equations given below are for the examples shown in Fig. 2.

A. Artery $$\Delta P_L = \frac{8\mu Q Z_e}{\pi r^4 \rho L} \tag{10}$$

B. Channels $$\Delta P_L = \frac{8\mu Q Z_e}{\pi r_e^4 N \rho L} \tag{11}$$

C. Screen $$\Delta P_L = \frac{b\mu Q Z_e}{\pi (R_W^2 - R^2)\, \epsilon\, r_c^2 \rho L} \quad (12)$$

D. Concentric Annulus $$\Delta P_L = \frac{12\mu Q Z_e}{\pi D W^3 \rho L} \quad (13)$$

E. Crescent Annulus $$\Delta P_L = \frac{4.8\mu Q Z_e}{\pi D W^3 \rho L} \quad (14)$$

The quantities are defined as follows:

Z_e = effective length of heat pipe
r_e = effective channel radius
N = number of channels
b = screen tortuosity factor
R_W = outer radius of screen structure
R = radius of vapor passage
ϵ = screen void fraction
r_c = effective radius of screen openings
D = mean diameter of annulus
w = width of annulus

Equations 10 through 14, except Eq. 12, are simple modifications of Eq. 9. In all cases, Q/L is substituted for $\dot{m}_L$, and Z_e for Z. The first substitution comes from Eq. 1 because $\dot{m}_L = \dot{m}_V$ in a heat pipe. The second substitution comes from the relationship

$$Z_e = \frac{Z_h + Z_c}{2} + Z_i, \quad (15)$$

where Z_h = heated length, Z_c = cooled length, and Z_i = insulated length between heated and cooled sections. When the middle of a heat pipe is heated and the remainder is cooled, the effective length is

$$Z_e = \frac{Z_h + Z_c}{4} . \quad (16)$$

Although the artery wick system appears ideal, it requires an additional capillary network to distribute the liquid over surfaces which are used for heat addition and removal. Because of this complication, arteries are usually reserved for systems where boiling is likely to occur within the wick if the bulk of the liquid-return network is located in the path of the incoming heat. (The consequences of such boiling will be discussed later.)

Equation 11 is essentially the same as Eq. 10, except that it involves a number of channels, N, and an effective channel radius, r_e, which is obtained by the hydraulic-radius method

$$r_e = 2\left(\frac{\text{Flow area}}{\text{Wetted perimeter}}\right) . \quad (17)$$

Although open channels are subject to an interaction of vapor and liquid, which causes waves but no liquid entrainment, the interaction can be suppressed by covering the channels with a layer of fine-mesh screen. Because the screen is located at the interface of liquid and vapor, the fine pores of the screen provide large capillary forces for fluid circulation, while the channels provide a less restrictive flow path for liquid return. This general type of structure is called a composite wick.

All-screen composite wicks can be made by wrapping a layer of fine screen around a mandrel followed by a second layer of coarse screen. The assembly can be placed in a container tube, the diameter of which is then drawn down until the inner wall makes contact with the coarse screen. The quantity $(b/\epsilon\, r_c^2)$ in Eq. 12 can next be determined by liquid-flow measurements through the screen before the mandrel is removed. Although the flow impedance of an all-screen wick can be controlled carefully, this was not done in early heat pipes so that Eq. 12 often appeared useless.

An ideal wick system for liquid-metal working fluids consists of an inner porous tube separated from an outer container tube by a gap which provides an unobstructed annulus for liquid return. The pressure drop in a concentric annulus (Eq. 13) is obtained by deriving Poiseuille's equation for flow between two parallel plates. Although not as precise as the equation for flow between concentric cylinders, it is easier to handle and is fairly accurate provided the width of the annulus is small compared to its mean diameter. Equation 14 for a crescent annulus is obtained by assuming the displacement obeys a

cosine function--the width of the annulus doubles at the top of the tube, becomes zero at the bottom, and remains unchanged on the sides.

In Fig. 1, the wicking limitation is represented by the solid line between Points 3 and 4. Although this limitation is shown to occur at temperatures where essentially all of the pressure drop is in the liquid phase, the effect of a significant vapor-pressure drop is indicated by the dotted extension line at lower temperatures.

Boiling Limitation

In most two-phase flow systems the formation of vapor bubbles in the liquid phase (boiling) enhances convection, which is required for heat transfer. Such boiling is often difficult to produce in liquid-metal systems because the liquid tends to fill the nucleation sites necessary for bubble formation. In a heat pipe, convection in the liquid is not required because heat enters the pipe by conduction through a thin saturated wick. Furthermore, the formation of vapor bubbles is undesirable because they could cause hot spots and destroy the action of the wick. Therefore, heat pipes are usually heated isothermally before being used to allow the liquid to wet the inner heat-pipe wall and to fill all but the smallest nucleation sites.

Although boiling has not been encountered in heat pipes with liquid-metal fluids, it may occur at high input heat fluxes and high operating temperatures. The curve between Points 4 and 5 in Fig. 1 is based on the equations

$$P_i - P_L = \frac{2\gamma}{r} \qquad (18)$$

$$\frac{Q}{S} = \frac{k(T_w - T_v)}{t} \quad , \qquad (19)$$

where P_i = vapor pressure inside bubble, P_L = pressure in adjacent liquid, r = radius of largest nucleation site, S = heat input area, k = effective thermal conductivity of saturated wick, T_w = temperature at inside wall, T_v = temperature at liquid-vapor interface, and t = wick thickness.

Since the sizes of nucleation sites in any system are usually unknown, it is not possible to predict when boiling will occur. However, Eqs. 18 and 19 show how various factors influence boiling. For example, if nucleation sites are small, a large pressure difference will be required for bubbles to grow. For a given heat-input flux, this pressure difference will depend on the thickness and thermal conductivity of the wick, on the saturation temperature of the vapor, and on the pressure drop in the vapor and liquid phases. This pressure drop is often overlooked because it is not a factor in the ordinary treatment of boiling.

When H_2O is used as the working fluid, boiling may be a major heat-transfer limitation because the thermal conductivity of the fluid is low and because it does not readily fill nucleation sites. Unfortunately, investigations of H_2O-operated heat pipes have largely ignored the boiling problem, and little experimental information is available concerning this limitation.

Bibliography

1. G. M. Grover, T. P. Cotter, and G. F. Erickson, "Structures of Very High Thermal Conductance," J. Appl. Phys. 35, 1990 (1964).
2. J. E. Deverall and J. E. Kemme, "High Thermal Conductance Devices Utilizing the Boiling of Lithium and Silver," Report LA-3211, Los Alamos Scientific Laboratory, 1965.
3. T. P. Cotter, "Theory of Heat Pipes," Report LA-3246-MS, 1965.
4. G. M. Grover, J. Bohdansky, C. A. Busse, "The Use of a New Heat Removal System in Space Thermionic Power Supplies," EUR 2229.e (EURATOM) 1965.
6. W. A. Ranken and J. E. Kemme, "Survey of Los Alamos and EURATOM Heat Pipe Investigations," IEEE Thermionic Conversion Specialist Conference, San Diego, 1965.
7. T. P. Cotter, "Status of Engineering Theory of Heat Pipes," Proceedings of Joint Atomic Energy Commission/Sandia Laboratories Heat Pipe Conference, SC-M-66-623, 1966.
8. J. E. Kemme, "Heat Pipe Capability Experiments," Report LA-3585-MS, 1966.
9. J. E. Deverall and E. W. Salmi, "Orbital Heat Pipe Experiment," Report LA-3714, 1967.
10. T. P. Cotter, "Heat Pipe Startup Dynamics," IEEE Thermionic Conversion Specialist Conference, Palo Alto, 1967.

11. J. E. Kemme, "High Performance Heat Pipes," IEEE Thermionic Conversion Specialist Conference, Palo Alto, 1967.

12. J. E. Deverall and E. W. Salmi, "Heat Pipe Performance in Space Environment," IEEE Thermionic Conversion Specialist Conference, Palo Alto, 1967.

13. J. E. Deverall, "The Effect of Vibration on Heat Pipe Performance," LA-3798, 1967.

14. J. E. Deverall, "Total Hemispherical Emissivity Measurements by the Heat Pipe Method," Report LA-3834-MS, April, 1968.

15. J. E. Kemme, "Ultimate Heat Pipe Performance," IEEE Thermionic Conversion Specialist Conference, Framingham, Mass., 1968.

16. J. E. Kemme, "Ultimate Heat Pipe Performance," (Revised), IEEE Transactions on Electron Devices, August, 1969.